Chemosphere 237 (2019) 124473

Contents lists available at ScienceDirect

Chemosphere

journal homepage: www.elsevier.com/locate/chemosphere

Assessment of membrane bioreactor fouling with the addition of suspended aluminum nitride nanoparticles

Lijie Zhou [a, *], Biao Ye [b, c], Siqing Xia [b, **]

[a] College of Chemistry and Environmental Engineering, Shenzhen University, Shenzhen, 518060, China
[b] State Key Laboratory of Pollution Control and Resource Reuse, College of Environmental Science and Engineering, Tongji University, 1239 Siping Road, Shanghai, 200092, China
[c] Shanghai Pudong Architectural Design & Research Institute, Shanghai, 201204, China

HIGHLIGHTS

- Suspended AlN NPs addition had no obvious effects on pollutant biodegradation.
- AlN NPs obviously increased membrane permeability and mitigated membrane fouling.
- AlN NPs led to thinner cake layer with inhibiting framework components accumulation.

GRAPHICAL ABSTRACT

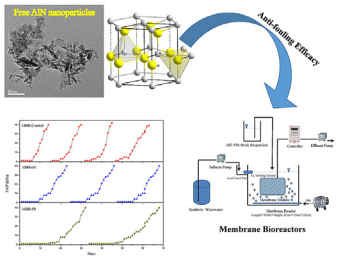

ARTICLE INFO

Article history:
Received 21 April 2019
Received in revised form
25 July 2019
Accepted 26 July 2019
Available online 29 July 2019

Handling Editor: A Adalberto Noyola

Keywords:
Suspended AlN nanoparticles
Fouling
Cake layer
Membrane bioreactor

ABSTRACT:

In this study, we assessed fouling in a membrane bioreactor (MBR) with the addition of suspended aluminum nitride (AlN) nanoparticles (NPs). Three parallel laboratory-scale submerged MBRs were operated with 0, 10, and 50 mg AlN NPs/L for over 70 days. The results showed that the addition of suspended AlN NPs did not significantly affect pollutant biodegradation; there was only a slight decrease in NH_4^+-N removal. Furthermore, the membrane's permeability was increased with effective fouling mitigation by the addition of a high amount of suspended AlN NPs. This was because the suspended AlN NPs decreased the content of polysaccharides in both the extracellular polymeric substances and soluble microbial products, and decreased the sludge floc size. However, the AlN NPs also promoted pore-blocking, particularly standard blocking, which enhanced irreversible fouling. Additionally, owing to the larger ionic radius and higher electronegativity, the AlN NPs inhibited the accumulation of framework components (SiO_2). Therefore, suspended AlN NPs resulted in a thinner cake layer.

1. Introduction

The rapid economic development in recent years has partly contributed to the development of megacities worldwide (such as Beijing, Guangzhou, and Sao Paulo) (Chen et al., 2018; Di Giulio et al., 2018), which require high-efficiency wastewater treatment with a small environmental footprint (Zhou et al., 2017a). Unlike other wastewater treatment technologies, membrane bioreactors (MBRs) are a promising and practical alternative for the stable and efficient treatment, as it has the advantages of high volumetric organic loading, excellent effluent quality, a small environmental footprint, and low sludge production (Meng et al., 2017). Large-

* Corresponding author.,
** Corresponding author.
E-mail addresses: pakerzhou@gmail.com, pakerzhou@szu.edu.cn (L. Zhou), siqingxia@gmail.com (S. Xia).

https://doi.org/10.1016/j.chemosphere.2019.124473
0045-6535/

scale MBR plants have been constructed and are under operation. The Wenyu River wastewater treatment plant (WWTP) in Beijing and the Jingxi WWTP in Guangzhou have both constructed super-large scale MBR systems with a capacity of 100000 m^3/d (Qin et al., 2018; Xiao et al., 2019). The Henriksdal WWTP in Sweden is expected to have a capacity of 864000 m^3/d, making it the largest MBR under construction (Xiao et al., 2019).

Membrane fouling is a major drawback and obstacle to the implementation of MBR systems, as it increases the operational costs and inhibits the promotion of MBR (Guo et al., 2012; Meng et al., 2017; Huang et al., 2019). Membrane fouling mainly involves pore-blocking and cake layer formation (Iorhemen et al., 2017). Previous literature reviews (Guo et al., 2012; Wang et al., 2013) found that the characteristics of activated sludge (such as the soluble microbial products (SMP), extracellular polymeric substances (EPS), and floc size) are the primary contributors to fouling development. Meng et al. (2017) also found that polysaccharides are the major organic components of the cake layer that forms during membrane fouling. Quorum quenching has been employed to inhibit bacterial communication and mitigate the characteristics of activated sludge, particularly SMP and EPS, that contribute to cake layer formation (Salehiziri et al., 2018; Huang et al., 2019). Additionally, the inorganic components, particularly metal elements of membrane fouling formation (such as Ca, Mg, Si, Al, and Fe), have also been studied, such as the function of SiO_2 in the formation of the cake layer framework (Guo et al., 2012; Meng et al., 2017). In our previous study (Zhou et al., 2017a), we assessed and discussed the effects of inorganic compounds on membrane fouling, particularly cake layer formation, and offered an identification process for the cake layer.

To mitigate membrane fouling, nanotechnology and nanoparticles (NPs), which have been widely applied in wastewater treatment (Xu et al., 2014; Xu and Hu, 2015), have been considered as an alternative anti-fouling technology, particularly for membrane modification (Gebru and Das, 2018). The nano-scale hydrophilic channels and decomposition of organic compounds by NPs both mitigate membrane fouling (Kim and Van der Bruggen, 2010; Qin et al., 2018). Previous studies (Kim and Van der Bruggen, 2010; Zhou et al., 2014b) reported that SiO_2 forms the framework of the cake layer, and TiO_2 NPs could replace the Si ions and coordinate with −COOH, mitigating membrane fouling. Therefore, NPs with similar structures to TiO_2 NPs could be an alternative anti-fouling technology. Aluminum nitride (AlN) NPs contain interpenetrating hexagonal closely-packed sublattices, which is similar to the structure of TiO_2 NPs. AlN NPs are widely applied in electronic substrates and steel; therefore, AlN NPs are a common industrial product, likely have a low price in the future. AlN NPs dissolve slowly in mineral acids as they attack the grain boundaries, and in strong alkalis as they attack the AlN grains (Lerner et al., 2016). Thus, it could be inferred that AlN NPs are a good alternative for mitigating fouling in MBR. However, the potential toxicity and effects of NPs on reactor performance during biological wastewater treatment have received more attention in recent years (He et al., 2017). Although nano zero-valent iron (NZVI) and TiO_2 NPs have been widely applied in wastewater treatment system (Kim and Van der Bruggen, 2010; Xu and Hu, 2015), the catalytic functions of NZVI and TiO_2 NPs cause organic compounds to decompose and damage bacterial metabolism, which finally decreases performance (Zhou et al., 2014b, 2017c; Zheng et al., 2015). Additionally, we found that AlN NPs have acute effects on the SMP of activated sludge in batch experiments with conical flasks in our previous study (Zhou et al., 2017b). According to a comparison of different NP toxicity studies (Zhou et al., 2014b; Zheng et al., 2015; Hou et al., 2017), the toxicity of NPs varies between different treatment systems. Consequently, before AlN NPs are applied in membrane fouling, their effects on membrane fouling, reactor performance, and bacterial metabolism should be considered and studied, particularly in their suspended form at a high concentration (Zheng et al., 2015).

In this study, we aimed to assess the fouling of MBR with the addition of suspended AlN NPs. This study was conducted following previous work on NP toxicity and membrane fouling (Zhou et al., 2014b, 2017b, 2017c; Zheng et al., 2015) to elucidate the possibility of applying AlN NPs for mitigating fouling. According to our previous study (Zhou et al., 2017b) on the acute effects of suspended AlN NPs, an AlN NP concentration of over 10 mg/L decreased the SMP of activated sludge from 56.65 to 48.88 mg/L, and the dehydrogenase of activated sludge was negatively related to the suspended AlN NPs concentration within a range of 1−200 mg/L. Additionally, a previous study (Zhou et al., 2017b) also reported that NPs significantly affect bacteria and membrane fouling at the mg/L level. Consequently, the AlN NPs concentrations studied here were 0 (control system), 10, and 50 mg/L to identify potential effects of AlN NPs on membrane fouling in a submerged MBR.

2. Materials and methods

2.1. AlN NPs suspension preparation

Commercial AlN NPs (A109771, Aladdin, China) were used in this study. The primary size of the AlN NPs in the stock suspension was approximately 50 nm. The AlN NPs stock suspension (100 mg/L) was prepared by adding 100 mg of AlN NPs to 1 L of Milli-Q water, followed by 1 h ultrasonication (25 °C, 300 W, 40 kHz), according to the literature (Keller et al., 2010).

2.2. Synthetic wastewater

The influent wastewater was prepared with deionized water according to previous work (Zhou et al., 2014b). The synthetic wastewater was stirred continuously and contained 420 mg/L of glucose, 420 mg/L of corn starch, 33 mg N/L of NH_4Cl, 11 mg/L of KH_2PO_4, 40 mg/L of SiO_2, 8 mg/L of $CaCl_2$, 9 mg/L of $MgSO_47H_2O$, 3.66 mg/L of $MnSO_4H_2O$, and 0.55 of $FeSO_47H_2O$. $NaHCO_3$ was used as a buffer to adjust the synthetic wastewater pH to approximately 7.0.

2.3. Set-up and operation of MBRs

Three parallel 3-L (working volume) submerged MBRs (the structure of the MBR is shown in Fig. S2; MBR-Control (without AlN NPs), MBR-10 (with 10 mg AlN NPs/L), and MBR-50 (with 50 mg AlN NPs/L)) were operated with synthetic wastewater for over 70 days. A hollow-fiber PVDF membrane module (total surface area of 0.02 m^2 and pore size of 0.1 μm, manufactured by Li-tree Company, Suzhou, China) was immersed in each MBR. Air (0.4 m^3/h) was continuously supplied through a perforated pipe located underneath the membrane module. A peristaltic pump equipped with a distributing pan was employed to control the influent feeding rate, and the hydraulic retention time (HRT) and sludge retention time (SRT) were maintained at 8.0 h and 30 days for each MBR, respectively. The intermittent suction mode (10 min of suction and 2 min of relaxation per cycle) was applied for flux control during each MBR operation cycle. When the trans-membrane pressure (TMP) reached 40 kPa, the membrane module was removed for physical (washing in tap water) and chemical cleaning (2% NaOCl and 1% citric acid immersion for 4 h, respectively) before the next cycle.

Inoculating sludge that had been pretreated with a phosphate buffer saline wash to remove the original Al was obtained from the Quyang WWTP (Shanghai, China) and added to each MBR. The

newly inoculated MBRs were initially operated to achieve a steady state to acclimate the activated sludge. The concentrations of Al in the sludge and influent were tested to ensure that there were no other Al sources in the reactor. MBR-10 and MBR-50 were then initially fed with an AlN NPs stock suspension (100 mg/L) to reach the predetermined AlN NPs concentration, and the operational time was recorded when the MBRs performance was stable. The AlN NPs were directly added into each reactor during operation, and the influent did not contain any AlN NPs or other Al components. As the concentration of AlN NPs in MBR-10 and MBR-50 could slowly decrease due to effluent or sludge discharge, a certain amount of the AlN NPs stock suspension (100 mg/L) was supplemented daily to maintain the initial AlN NPs concentration after determining the total AlN concentration of the mixed liquid, which was conducted after nitric acid digestion, because AlN was the only aluminum source in this experiment. MBR-Control was operated as the control unit, without any AlN NPs.

2.4. Membrane resistance analysis

The membrane resistance of fouling was measured and calculated based on the following equations (Zhou et al., 2015a):

$$R_{total} = R_{clean\ membrane} + R_{pore\ blocking} + R_{cake\ layer} \quad (1)$$

$$R_n = \frac{\triangle P}{\mu J} \quad (2)$$

where $R_{clean\ membrane}$ is the resistance of the clean membrane (new or post-cleaning membrane modules were regarded as clean membranes), $R_{pore\ blocking}$ is the resistance due to pore-blocking, and $R_{cake\ layer}$ is the cake layer's resistance. The resistance of concentration polarization was considered as part of $R_{cake\ layer}$ in this study (Meng et al., 2007). R_n is the total, clean membrane, pore-blocking, or cake layer resistance, $\triangle P$ is the TMP, J is the permeate flux, μ is the viscosity of the permeate water, and R_{total} is the sum of $R_{clean\ membrane}$, $R_{pore\ blocking}$ and $R_{cake\ layer}$. R_{total}, $R_{clean\ membrane}$, and $R_{pore\ blocking}$ were measured and calculated according to equation (2), while $R_{cake\ layer}$ was calculated according to equation (1).

2.5. Extraction and measurement of SMP and EPS

SMP and EPS were extracted following modified thermal extraction methods described in previous work (Zhou et al., 2017b, 2017c). SMP and EPS were normalized as the polysaccharide and protein concentrations, and were measured following the phenol-sulfuric acid and Branford methods, respectively (Zhou et al., 2014a; Salehiziri et al., 2018). The inorganic components of the cake layer were extracted following previous methods (Zhou et al., 2014b) and measured following the same process as EPS.

2.6. Silt density index measurement

Silt density index (SDI) analysis was conducted according to the ASTM D4189-95 standards (Koo et al., 2012). The mixed liquor was pumped through a 0.45-μm membrane with an in-line filter holder at a constant pressure of 207 kPa in the dead-end flow mode. The SDI value was calculated based on Eq. (2):

$$\mathrm{SDI} = \frac{1 - \frac{t_i}{t_f}}{15} \times 100 \quad (2)$$

where t_i and t_f are the times at which the initial and final 500 mL of mixed liquor were collected, respectively.

2.7. Other analytical methods

The ammonia nitrogen (NH_4^+-N), chemical oxygen demand (COD), total phosphorus (TP), total nitrogen (TN), mixed liquor suspended solids (MLSS), and mixed liquor volatile suspended solids (MLVSS) contents were detected following standard methods (China-NEPA, 2002). The concentrations of AlN NPs in the supernatant and mixed liquid were analyzed via an inductively coupled plasma-optical emission spectrometer (ICP-OES, Optima 2100 DV, PerkinElmer, USA) according to Zhou et al. (2017b). The functional groups of the activated sludge were determined by conducting FTIR spectroscopy analysis (Nicolet 5700, Thermo, USA) after 48 h of freeze-drying as pretreatment. The FTIR spectra were measured at wavenumbers in the range of 4000−400 cm^{-1} with a resolution of 4 cm^{-1}. A sample of the fouled membrane was cut from the membrane module at 40 kPa TMP, and the thickness and elemental distribution of the cake layer on this sample were measured through SEM (XL30, Philips, Netherlands)-EDX (Oxford Isis, UK) after liquid N_2 pretreatment.

3. Results and discussion

3.1. Reactor performance and membrane permeability

The variations in the performances of MBR-Control, MBR-10, and MBR-50 are shown in Table 1. Over 90% of the COD was removed with or without AlN NPs. The NH_4^+-N removal efficiency only decreased by 5% with the addition of suspended AlN NPs, while the MLSS and MLVSS contents both decreased significantly with the addition of AlN NPs (Table 2), indicating that the activated sludge viability had decreased, which directly inhibited NH_4^+-N removal. Zheng et al. (2016) demonstrated that nano-scale particles damaged the integrity of membranes used for reducing dehydrogenase in activated sludge. Furthermore, previous studies (Chen et al., 2015; Zheng et al., 2015; He et al., 2017) reported that NPs would also affect the key functional genes and enzyme activity of bacteria. Additionally, during the whole operation, mixed liquor of both MBR-10 and MBR-50 contained less than 0.1 mg/L of Al^{n+}, and the concentrations of insoluble Al exceeded 9.8 and 49.7 mg/L, respectively, indicating that few AlN NPs transformed into Al^{n+} during operation and should not decrease the NH_4^+-N removal efficiency. Therefore, the decrease in the removal of NH_4^+-N with the addition of suspended AlN NPs should be due to the size of the AlN NPs. Moreover, the variations in the removal of TN and TP with the addition of suspended AlN NPs by the MBRs were minimal. The performances of the reactors indicated that the addition of suspended AlN NPs did not significantly affect pollutant biodegradation.

Fig. 1 presents the variations in the TMP of the MBRs to identify the effects of suspended AlN NPs on the permeability and fouling of the membranes. TMP variation is classified into two-stages: slight initial TMP increase, and TMP jump (Zhou et al., 2014b). In the first stage, the slight increase in TMP is caused by the blocking of pores on the surface of the membrane, followed by the initial cake layer formation. In the second stage, the TMP jump is caused by the cake layer on the membrane's surface (He et al., 2016). As shown in Fig. 1, the initial slight TMP increase stage was postponed with the addition of suspended AlN NPs. During the TMP jump stage, the TMP increase rates (dTMP/dt) of MBR-Control, MBR-10, and MBR-50 remained at 3.0, 3.3, and 5.1 kPa/d, respectively, indicating that the addition of suspended AlN NPs mitigated membrane fouling and increased the membrane's permeability. Moreover, the membrane was cleaned according to the typical protocol for cleaning this membrane module supplied by the membrane's manufacturer. Our membrane cleaning procedure was similar to that followed in

Table 1
Average characteristics of the influent and effluent water. All the values represent mean ± SD (n = 70).

Parameters	MBR-Control			MBR-10			MBR-50		
	Influent (mg/L)	Effluent (mg/L)	Removal (%)	Influent (mg/L)	Effluent (mg/L)	Removal (%)	Influent (mg/L)	Effluent (mg/L)	Removal (%)
COD	510 ± 25	29 ± 3	94 ± 2	495 ± 45	4 ± 1	99 ± 4	509 ± 45	3 ± 1	99 ± 1
NH_4^+-N	44.9 ± 1	0.7 ± 0.3	98 ± 1	44.2 ± 3	3.3 ± 1.2	93 ± 2	45.2 ± 1	3.6 ± 0.6	92 ± 1
TN	33 ± 2	23 ± 4	33 ± 4	32 ± 3	24 ± 2	32 ± 4	33 ± 3	25 ± 5	30 ± 4
TP	2.5 ± 2	2 ± 1	20 ± 3	2.5 ± 2	1.8 ± 1	28 ± 4	2.5 ± 2	2.1 ± 1	16 ± 3

a. Each item was analyzed every day.
b. MLSS (n = 8): MBR-Control 4500 ± 200 mg/L; MBR-10 3700 ± 300 mg/L; MBR-50 4000 ± 300 mg/L.

Table 2
Analysis results of clean membrane resistance ($R_{clean\ membrane}$), pore-blocking resistance ($R_{pore\ blocking}$), cake resistance ($R_{cake\ layer}$), and total resistance (R_{total}).[a]

Item	MBR-Control [a]		MBR-10 [b]		MBR-50 [c]	
	Value ($10^{12}m^{-1}$)	Percentage (%)	Value ($10^{12}m^{-1}$)	Percentage (%)	Value ($10^{12}m^{-1}$)	Percentage (%)
$R_{clean\ membrane}$ [b]	0.23 ± 0.02	2.1 ± 0.34	0.33 ± 0.08	6 ± 0.51	0.33 ± 0.05	7 ± 0.82
$R_{pore\ blocking}$	0.27 ± 0.03	4.5 ± 0.83	0.77 ± 0.28	13 ± 0.85	0.62 ± 0.09	13 ± 1.5
$R_{cake\ layer}$	10.30 ± 0.88	95.4 ± 2.5	4.61 ± 0.59	81 ± 1.5	3.66 ± 0.28	80 ± 3.8
R_{total}	10.80 ± 1.08	–	5.71±	–	4.61±	–

[a] Membrane resistance was analyzed thrice when TMP = 40 kPa; a: n = 6; b: n = 9; c: n = 12.
[b] The $R_{clean\ membrane}$ of the whole new membrane module (without any use) was 0.19 ± 0.01 $10^{12}m^{-1}$. The $R_{clean\ membrane}$ in Table 2 was the average value calculated from each membrane resistance data, meaning that $R_{clean\ membrane}$ presented the irreversible fouling caused by last membrane operation.

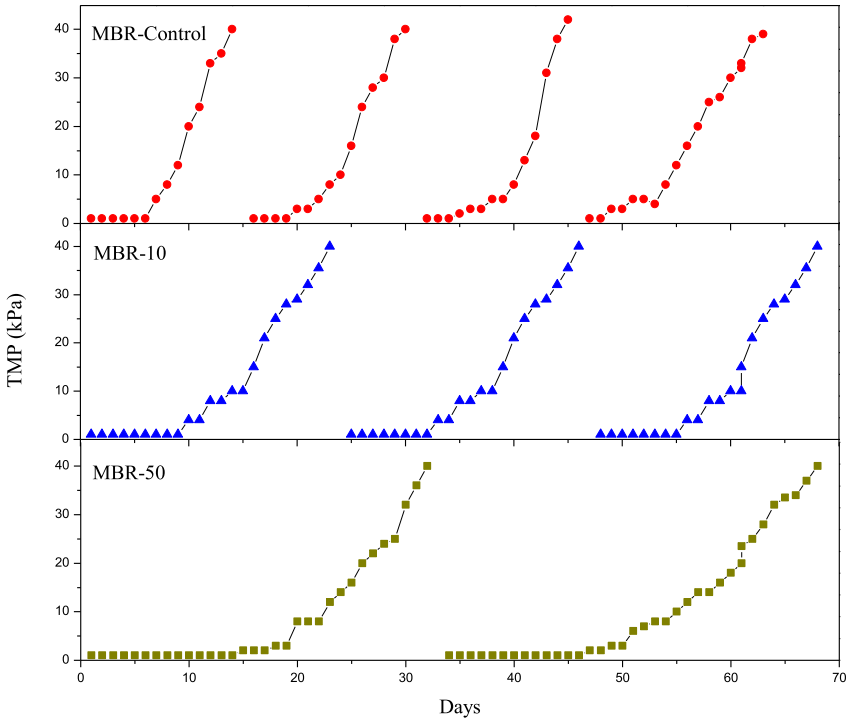

Fig. 1. TMP variations of MBRs during operation. (When the TMP reached 40 kPa, the membrane module was removed for physical (tap water washing) and chemical cleaning (2% NaOCl and 1% citric acid immersion for 4 h, respectively prior to the next run.). The membrane module was washed with deionized water until no Al was detected from the washing water.).

practice, thus, the membrane cleaning result should be close to that endured in the real operational lifetime of a membrane module. Fig. 1 shows that the AlN NPs were positively related to the time required for membrane cleaning. Therefore, AlN NPs improved the operational lifetime of the membrane module and mitigated the total membrane fouling.

As shown in Table 2, fouling resistance was calculated using the permeation data and resistance-in-series model (Johir et al., 2013). With the addition of suspended AlN NPs, the total resistance (R_{total}) and cake resistance ($R_{cake\ layer}$) decreased notably, indicating that the addition of suspended AlN NPs effectively mitigated membrane fouling, particularly by a cake layer. However, the addition of suspended AlN NPs also increased the pore-blocking resistance, indicating severe pore-blocking. This could be due to the nano-size and high adsorbability of suspended AlN NPs. Membrane fouling typically occurs due to pore-blocking and cake layer formation (Guo et al., 2012). Moreover, $R_{clean\ membrane}$, which predicts the irreversible fouling caused by the previous membrane operation cycle, was

0.23 ± 0.02, 0.33 ± 0.08, and 0.33 ± 0.05 $10^{12}m^{-1}$ in MBR-Control, MBR-10 and MBR-50, respectively, while that of the new membrane module was 0.19 ± 0.01 $10^{12}m^{-1}$, indicating severe irreversible fouling by the addition of AlN NPs. According to previous literature (Le-Clech et al., 2006; Meng et al., 2009; Wang et al., 2013), pore-blocking mainly contributes to irreversible fouling during MBR operation, although cake layer formation is the main fouling process. Wang and Tarabara (2008) classified pore-blocking into complete, standard, and intermediate blocking. Unlike complete and intermediate blocking, standard blocking is not easily removed through physical and chemical cleaning, and likely directly causes irreversible fouling. The intermediate blocking mechanism is similar to that of cake layer fouling. Therefore, according to the $R_{clean\ membrane}$ data, the addition of AlN NPs could promote pore-blocking, particularly standard blocking, leading to severe, irreversible fouling. According to Fig. 1 and Table 2, AlN NPs could effectively mitigate membrane fouling and cake layer formation, but aggravate pore-blocking. Therefore, membrane fouling was mainly mitigated by the addition of suspended AlN NPs due to the inhibition of cake layer formation.

3.2. Activated sludge characteristics associated with membrane fouling

The activated sludge characteristics associated with membrane fouling were also investigated. The FTIR spectrogram (Fig. S3(a)) presents the functional groups of the bacteria and AlN NPs. The similar FTIR of the activated sludge with and without the addition of suspended AlN NPs indicated that the suspended AlN NPs would not affect the major functional groups of the sludge. A peak at 495 cm^{-1} was found in the activated sludge with the suspended AlN NPs, indicating that the AlN NPs combined with activated sludge in the form of an Al—O bond (Gupta et al., 2011).

The SMP and EPS of activated sludge are the key components of membrane fouling (Zhou et al., 2015b; Meng et al., 2017). As shown in Table 3, the suspended AlN NPs did not notably affect the protein of both SMP and EPS during MBR operation, which was consistent with the results of previous work (Zhou et al., 2017b), and only led to a slight decrease in the content of EPS protein. Kumar and Nussinov (2001) reported that the repulsive electrostatic interactions, restricted set of conformations, and shape complementarity of hydrophobic residues maintain the protein's structure. However, the structure of proteins is easily disrupted by the NPs that interact with the protein's surface owing to their nano-size (Lynch and Dawson, 2008). Moreover, unlike heavy metal NPs (such as CuO NPs, Ag NPs (Grun et al., 2016; Miao et al., 2017)), the toxicity of AlN NPs is mainly due to their size, and not the toxicity of the metal. Thus, bacteria are unlikely to produce more protein with the addition of AlN NPs. Consequently, AlN NPs did not significantly affect the protein contents of both SMP and EPS, only causing a slight decrease in the EPS protein content. Additionally, AlN NPs effectively reduced the polysaccharide contents of both SMP and EPS, with the polysaccharide content of SMP decreasing from 62 to 43 mg/L due to the addition of AlN NPs. Philippe and Schaumann (2014) stated that Al NPs easily adsorb to the surface of polysaccharides due to van der Waals and hydrophobic forces, as well as the carboxyl and hydroxyl groups. Although proteins interacted with NPs in a similar manner to polysaccharides, the variations in the protein contents depended on the protection of bacteria against the toxicity of NPs, particularly the metallic toxicity (Hou et al., 2017; Miao et al., 2017). Therefore, AlN NPs with low metallic toxicity mainly decreased the polysaccharide content. Furthermore, polysaccharides are the key organic components contributing to membrane fouling (Meng et al., 2017), and the decrease in polysaccharides partly contributed to the mitigation of membrane fouling by the suspended AlN NPs.

The particle size distribution (PSD) of activated sludge flocs was also positively correlated with membrane fouling (Salih et al., 2015). Fig. S3(b) presents the variations in the PSD of activated sludge between three MBRs. The addition of AlN NPs reduced the average particle size from 52 to 10 μm. Many experimental studies (Wang et al., 2008; Lin et al., 2011) demonstrated that small flocs had a strong tendency to adhere to the membrane's surface and easily blocked the membrane pores, increasing pore-blocking. This was consistent with the membrane resistance results. The activated sludge flocs decreased in size because the suspended AlN NPs absorbed onto the flocs' surfaces through the bidentate coordination of —COOH, which would inhibit the connection of flocs and mitigate cake layer formation (Zhou et al., 2017c).

3.3. Cake layer structure

Previous studies (Guo et al., 2012; Meng et al., 2017) reported that the cake layer plays a significant role in membrane fouling during MBR operation. Fig. S4 shows the variations in the thickness of the cake layer in each MBR. At an AlN NPs concentration of 50 mg/L, the cake layer thickness decreased from 84 μm (MBR-Control) and 85 μm (MBR-10) to 47 μm (MBR-50). The high concentration of suspended AlN NPs effectively reduced the thickness and re-structured the cake layer. Table 3 shows that the AlN NPs only decreased the polysaccharide content of the cake layer and did not significantly affect the proteins, which was consistent with the results of SMP and EPS. SMP and EPS have both been reported to contribute to cake layer formation (Guo et al., 2012; Meng et al., 2017). Similar reasons to those mentioned in Section 3.2 about SMP and EPS also contributed to the decrease in the polysaccharide content and did not significantly affect the protein content of the cake layer. Therefore, the addition of suspended AlN NPs mainly reduced the polysaccharide concentration of the cake layer. Additionally, the SDI values, which indicate the fouling tendency of MLSS, in MBR-Control, MBR-10, and MBR-50 were 3.8, 3.4, and 3.2, respectively. This indicates that the fouling tendency of MLSS decreased with the addition of AlN NPs, mitigating membrane fouling.

Previous studies (Zhou et al., 2014b, 2017c) demonstrated that NPs typically significantly affect the inorganic components of the cake layer. Mg, Al, Si, Ca, and Fe constitute the majority of inorganic components in the cake layer (Guo et al., 2012; Trzcinski and

Table 3
Variations of SMP (mg/L), EPS (mg/g MLVSS) and cake layer (mg/g cake layer) in each MBR. (n = 14) [a].

	SMP		EPS		Cake layer	
	Polysaccharide	Protein	Polysaccharide	Protein	Polysaccharide	Protein
MBR-Control	62 ± 5	16 ± 3	78 ± 8	26 ± 4	83 ± 3	42 ± 6
MBR-10	43 ± 4	14 ± 5	57 ± 7	28 ± 4	63 ± 6	43 ± 3
MBR-50	45 ± 8	18 ± 4	53 ± 5	24 ± 2	57 ± 7	39 ± 7

[a] Each item was analyzed every 10 days.

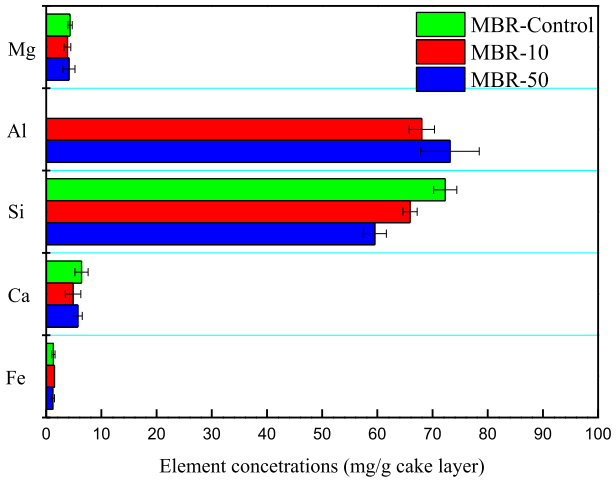

Fig. 2. Concentrations of inorganic elements in cake layer. (Each sample of cake layer was measured thrice when TMP = 40 kPa; n of MBR-Control = 6; n of MBR-10 = 9; n of MBR-50 = 12).

Stuckey, 2016). As mentioned in Section 3.1, few AlN NPs were transformed into Al^{n+} during operation. Therefore, AlN remained in the form of crystal AlN particles. The Si contents of the cake layers of MBR-Control, MBR-10, and MBR-50 were 72.3, 65.9, and 59.5 mg/g, respectively (Fig. 2), and Si mainly existed as crystal SiO_2, which constituted the majority of inorganic crystal particles in the cake layer (Zhou et al., 2015a). Fig. 2 further shows that Al and Si were the major inorganic components of the cake layer in each MBR, and the addition of suspended AlN NPs increased the Al concentration of the cake layer, but decreased the concentration of Si. Moreover, cross-sectional distributions of Al and Si in the cake layer are shown in Fig. 3 and S4, respectively. The AlN NPs were the only source of aluminum in this study, thus, the Al distribution in Fig. 3 represents the AlN NPs distribution along the cake layer. The mixed liquor in both MBR-10 and MBR-50 contained less than 0.1 mg/L Al^{n+}, and the concentrations of insoluble Al exceeded 9.8 and 49.7 mg/L, respectively. As shown in Fig. 3, crystal AlN NP accumulated on the cake layer with an increase in the AlN NPs content, but the cake layer thickness significantly decreased, indicating that the higher AlN NPs content resulted in a thinner cake layer. Fig. 3 also shows that AlN NPs accumulated on the cake layer, particularly during the later stages of membrane fouling. Additionally, SiO_2 forms the framework of the cake layer (Zhou et al., 2015a). Fig. S4 shows that the abundance of SiO_2 in the cake layer decreased, and its formation shifted from the beginning of operation to the later membrane fouling stage, indicating that the addition of suspended AlN NPs inhibited the accumulation of SiO_2 on the cake layer, and mitigated Si accumulation during the initial formation of the cake layer. According to previous work (Kim and Van der Bruggen, 2010) and the FTIR results, AlN and SiO_2 both connect to the organic components in the bidentate coordination of −COOH (Fig. 4). According to crystal chemistry (Chen, 2010), the aluminum in AlN (with a stable atomic structure) has a larger ionic radius and higher electronegativity than the silicon in SiO_2. Consequently, it is easier for aluminum to react with the functional groups (such as −COOH and −OH) of organic compounds and attach to the membrane's surface. Moreover, van der Waals and hydrophobic forces enhance the absorption of Al NPs to the surface of organic components, particularly polysaccharides (Philippe and Schaumann, 2014). Influent containing 40 mg/L of SiO_2 was continuously added to MBR-10 and MBR-50 for supplementing silicon, and the concentration of AlN NPs (sole Al source) in the MBRs was maintained. The organic compounds had previously interacted with AlN NPs, mitigating the contribution of SiO_2 to cake layer formation. However, SiO_2 still accumulated on the cake layer due to the continuous supplementation with Si. Therefore, the addition of suspended AlN NPs addition not only to cake layer formation, but also decreased the thickness of the cake layer by inhibiting the accumulation of framework components (SiO_2), further mitigating fouling.

4. Conclusions

In this study, the fouling of MBR with the addition of suspended AlN NPs was assessed. The addition of suspended AlN NPs did not significantly affect pollutant biodegradation, however, it clearly increased membrane permeability and mitigated membrane fouling. Furthermore, the addition of suspended AlN NPs effectively reduced the polysaccharide contents of both EPS and SMP, and

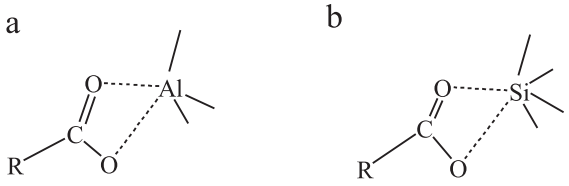

Fig. 4. Bidentate coordination of −COOH to (a) AlN and (b) SiO_2.

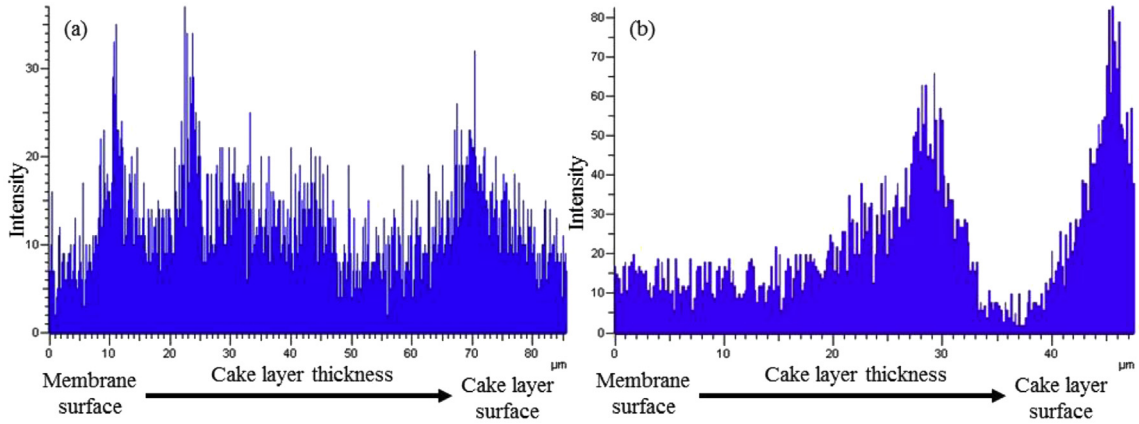

Fig. 3. The Al cross-sectional distribution of membrane foulant in (a) MBR-10 and (b) MBR-50. (x-axis (μm) presented the thickness of cake layer; y-axis (no unit) presented the intensity of Al. Sample was analyzed when TMP = 40 kPa. During analysis, 5 different points were measured, and the most representative result was shown.).

decreased the activated sludge floc size, further hindering the combination of sludge flocs and slowing membrane fouling. Additionally, the addition of suspended AlN NPs addition contributed to cake layer formation and reduced the cake layer's thickness by inhibiting the accumulation of framework components (SiO_2).

Acknowledgements

This study was funded by “Project 51708362 supported by National Natural Science Foundation of China”, “Natural Science Foundation of Shenzhen University (827-000282)”, “National Key Research and Development Program of China (2017YFC0403403)”, “New Teacher Natural Science Research Project of Shenzhen University (85303-00000135)” and “State Key Laboratory of Pollution Control and Resource Reuse Foundation (NO. PCRRF17025)”.

Appendix A. Supplementary data

Supplementary data to this article can be found online at https://doi.org/10.1016/j.chemosphere.2019.124473.

References

Chen, C., LeGates, R., Zhao, M., Fang, C., 2018. The changing rural-urban divide in China's megacities. Cities 81, 81–90.
Chen, H., Li, X., Chen, Y.G., Liu, Y.A., Zhang, H., Xue, G., 2015. Performance of wastewater biological phosphorus removal under long-term exposure to CuNPs: adapting toxicity via microbial community structure adjustment. RSC Adv. 5, 61094–61102.
Chen, J.Z. (Ed.), 2010. Modern Crystal Chemisty. Science Press, Beijing.
China-NEPA (Ed.), 2002. Water and Wastewater Monitoring Methods. Chinese Enviromental Science Publishing House, Beijing, China.
Di Giulio, G.M., Bedran-Martins, A.M.B., Vasconcellos, M.d.P., Ribeiro, W.C., Lemos, M.C., 2018. Mainstreaming climate adaptation in the megacity of São Paulo, Brazil. Cities 72, 237–244.
Gebru, K.A., Das, C., 2018. Removal of chromium (VI) ions from aqueous solutions using amine-impregnated TiO2 nanoparticles modified cellulose acetate membranes. Chemosphere 191, 673–684.
Grun, A.Y., Meier, J., Metreveli, G., Schaumann, G.E., Manz, W., 2016. Sublethal concentrations of silver nanoparticles affect the mechanical stability of biofilms. Environ. Sci. Pollut. Control Ser. 23, 24277–24288.
Guo, W.S., Ngo, H.H., Li, J.X., 2012. A mini-review on membrane fouling. Bioresour. Technol. 122, 27–34.
Gupta, V.K., Agarwal, S., Saleh, T.A., 2011. Synthesis and characterization of alumina-coated carbon nanotubes and their application for lead removal. J. Hazard Mater. 185, 17–23.
He, C.-S., He, P.-P., Yang, H.-Y., Li, L.-L., Lin, Y., Mu, Y., Yu, H.-Q., 2017. Impact of zero-valent iron nanoparticles on the activity of anaerobic granular sludge: from macroscopic to microcosmic investigation. Water Res. 127, 32–40.
He, Z.W., Miller, D.J., Kasemset, S., Wang, L., Paul, D.R., Freeman, B.D., 2016. Fouling propensity of a poly(vinylidene fluoride) microfiltration membrane to several model oil/water emulsions. J. Membr. Sci. 514, 659–670.
Hou, J., Yang, Y.Y., Wang, P.F., Wang, C., Miao, L.Z., Wang, X., Lv, B.W., You, G.X., Liu, Z.L., 2017. Effects of CeO2, CuO, and ZnO nanoparticles on physiological features of Microcystis aeruginosa and the production and composition of extracellular polymeric substances. Environ. Sci. Pollut. Control Ser. 24, 226–235.
Huang, J.H., Gu, Y.L., Zeng, G.M., Yang, Y., Ouyang, Y.C., Shi, L.X., Shi, Y.H., Yi, K.X., 2019. Control of indigenous quorum quenching bacteria on membrane biofouling in a short-period. MBR. Bioresour. Technol. 283, 261–269.
Iorhemen, O.T., Hamza, R.A., Tay, J.H., 2017. Membrane fouling control in membrane bioreactors (MBRs) using granular materials. Bioresour. Technol. 240, 9–24.
Johir, M.A., Shanmuganathan, S., Vigneswaran, S., Kandasamy, J., 2013. Performance of submerged membrane bioreactor (SMBR) with and without the addition of the different particle sizes of GAC as suspended medium. Bioresour. Technol. 141, 13–18.
Keller, A.A., Wang, H.T., Zhou, D.X., Lenihan, H.S., Cherr, G., Cardinale, B.J., Miller, R., Ji, Z.X., 2010. Stability and aggregation of metal oxide nanoparticles in natural aqueous matrices. Environ. Sci. Technol. 44, 1962–1967.
Kim, J., Van der Bruggen, B., 2010. The use of nanoparticles in polymeric and ceramic membrane structures: review of manufacturing procedures and performance improvement for water treatment. Environ. Pollut. 158, 2335–2349.
Koo, C.H., Mohammad, A.W., Suja, F., Talib, M.Z.M., 2012. Review of the effect of selected physicochemical factors on membrane fouling propensity based on fouling indices. Desalination 287, 167–177.
Kumar, S., Nussinov, R., 2001. How do thermophilic proteins deal with heat? Cell. Mol. Life Sci. CMLS 58, 1216–1233.
Le-Clech, P., Chen, V., Fane, T.A.G., 2006. Fouling in membrane bioreactors used in wastewater treatment. J. Membr. Sci. 284, 17–53.
Lerner, M.I., Lozhkomoev, A.S., Pervikov, A.V., Bakina, O.V., 2016. Synthesis of Al-Al2O3 and Al-Aln nanoparticle composites via electric explosion of wires. Russ. Phys. J. 59, 422–429.
Lin, H.J., Liao, B.Q., Chen, J.R., Gao, W.J., Wang, L.M., Wang, F.Y., Lu, X.F., 2011. New insights into membrane fouling in a submerged anaerobic membrane bioreactor based on characterization of cake sludge and bulk sludge. Bioresour. Technol. 102, 2373–2379.
Lynch, I., Dawson, K.A., 2008. Protein-nanoparticle interactions. Nano Today 3, 40–47.
Meng, F.G., Chae, S.R., Drews, A., Kraume, M., Shin, H.S., Yang, F.L., 2009. Recent advances in membrane bioreactors (MBRs): membrane fouling and membrane material. Water Res. 43, 1489–1512.
Meng, F.G., Zhang, H.M., Yang, F.L., Liu, L.F., 2007. Characterization of cake layer in submerged membrane bioreactor. Environ. Sci. Technol. 41, 4065–4070.
Meng, F.G., Zhang, S.Q., Oh, Y., Zhou, Z.B., Shin, H.S., Chae, S.R., 2017. Fouling in membrane bioreactors: an updated review. Water Res. 114, 151–180.
Miao, L.Z., Wang, C., Hou, J., Wang, P.F., Ao, Y.H., Li, Y., Yao, Y., Lv, B.W., Yang, Y.Y., You, G.X., Xu, Y., Gu, Q.H., 2017. Response of wastewater biofilm to CuO nanoparticle exposure in terms of extracellular polymeric substances and microbial community structure. Sci. Total Environ. 579, 588–597.
Philippe, A., Schaumann, G.E., 2014. Interactions of dissolved organic matter with natural and engineered inorganic colloids: a review. Environ. Sci. Technol. 48, 8946–8962.
Qin, L., Zhang, Y., Xu, Z., Zhang, G., 2018. Advanced membrane bioreactors systems: new materials and hybrid process design. Bioresour. Technol. 269, 476–488.
Salehiziri, M., Rad, H.A., Novak, J.T., 2018. Preliminary investigation of quorum quenching effects on sludge quantity and quality of activated sludge process. Chemosphere 209, 525–533.
Salih, H.H., Wang, L.X., Patel, V., Namboodiri, V., Rajagopalan, K., 2015. The utilization of forward osmosis for coal tailings dewatering. Miner. Eng. 81, 142–148.
Trzcinski, A.P., Stuckey, D.C., 2016. Inorganic fouling of an anaerobic membrane bioreactor treating leachate from the organic fraction of municipal solid waste (OFMSW) and a polishing aerobic membrane bioreactor. Bioresour. Technol. 204, 17–25.
Wang, F., Tarabara, V.V., 2008. Pore blocking mechanisms during early stages of membrane fouling by colloids. J. Colloid Interface Sci. 328, 464–469.
Wang, Z.W., Mei, X.J., Ma, J.X., Grasmick, A., Wu, Z.C., 2013. Potential foulants and fouling indicators in MBRs: a critical review. Separ. Sci. Technol. 48, 22–50.
Wang, Z.W., Wu, Z.C., Yin, X., Tian, L.M., 2008. Membrane fouling in a submerged membrane bioreactor (MBR) under sub-critical flux operation: membrane foulant and gel layer characterization. J. Membr. Sci. 325, 238–244.
Xiao, K., Liang, S., Wang, X., Chen, C., Huang, X., 2019. Current state and challenges of full-scale membrane bioreactor applications: a critical review. Bioresour. Technol. 271, 473–481.
Xu, S.N., Hu, Z.Q., 2015. Kinetics of nutrient removal by nano zero-valent iron under different biochemical environments. Water Environ. Res. 87, 483–490.
Xu, S.N., Sun, M.H., Zhang, C.Q., Surampalli, R., Hu, Z.Q., 2014. Filamentous sludge bulking control by nano zero-valent iron in activated sludge treatment systems. Environ. Sci. Process. Impact 16, 2721–2728.
Zheng, X., Huang, H.N., Su, Y.L., Wei, Y.Y., Chen, Y.G., 2015. Long-term effects of engineered nanoparticles on enzyme activity and functional bacteria in wastewater treatment plants. Water Sci. Technol. 72, 99–105.
Zheng, X., Su, Y.L., Chen, Y.G., Wan, R., Li, M., Huang, H.N., Li, X., 2016. Carbon nanotubes affect the toxicity of CuO nanoparticles to denitrification in marine sediments by altering cellular internalization of nanoparticle. Sci. Rep. 6.
Zhou, L., Xia, S., Alvarez-Cohen, L., 2015a. Structure and distribution of inorganic components in the cake layer of a membrane bioreactor treating municipal wastewater. Bioresour. Technol. 196, 586–591.
Zhou, L., Ye, B., Xia, S., 2017a. Assessing membrane biofouling and its gel layer of anoxic/oxic membrane bioreactor for megacity municipal wastewater treatment during plum rain season in Yangtze River Delta, China. Water Res. 127, 22–31.
Zhou, L., Zhang, Z., Jiang, W., Guo, W., Ngo, H.-H., Meng, X., Fan, J., Zhao, J., Xia, S., 2014a. Effects of low-concentration Cr (VI) on the performance and the membrane fouling of a submerged membrane bioreactor in the treatment of municipal wastewater. Biofouling 30, 105–114.
Zhou, L., Zhang, Z., Xia, S., Jiang, W., Ye, B., Xu, X., Gu, Z., Guo, W., Ngo, H.-H., Meng, X., 2014b. Effects of suspended titanium dioxide nanoparticles on cake layer formation in submerged membrane bioreactor. Bioresour. Technol. 152, 101–106.
Zhou, L., Zhuang, W., Wang, X., Yu, K., Yang, S., Xia, S., 2017b. Potential acute effects of suspended aluminum nitride (AlN) nanoparticles on soluble microbial products (SMP) of activated sludge. J. Environ. Sci. 57, 284–292.
Zhou, L.J., Zhuang, W.Q., Wang, X., Yu, K., Yang, S.F., Xia, S.Q., 2017c. Potential effects of loading nano zero valent iron discharged on membrane fouling in an anoxic/oxic membrane bioreactor. Water Res. 111, 140–146.
Zhou, Z.B., Meng, F.G., He, X., Chae, S.R., An, Y.J., Jia, X.S., 2015b. Metaproteomic analysis of biocake proteins to understand membrane fouling in a submerged membrane bioreactor. Environ. Sci. Technol. 49, 1068–1077.